1 Introduction

Since the discovery of electroluminescence in organic materials in 1955 by Bernanose[1], enormous progress has been made in enhancing efficiencies for electric devices based on organic semiconductors like organic light emitting diodes (OLEDs). The first OLED was already realized by Helfrich et al. in 1965[2]. As the antracen crystals used in this work were several microns in thickness, operating voltages of several hundred volts were required. The breakthrough came with Tang and vanSlyke, who presented the first organic light emitting thin film device based on organic small molecules deposited via thermal evaporation in 1987[3]. The bilayer structure of diamine and Alq_3[1] had operating voltages below $5\,\mathrm{V}$, making the field of organic electronics also interesting for technical applications. Since then, the efficiency increased continuously and products based on organic semiconductors finally captured the market. Nowadays, for example cell phones are equipped with OLED displays and also curved OLED TVs are already commercially available.

Even though the semiconductor industry is still dominated by inorganic materials like silicon or gallium arsenide, organic semiconductors have outstanding properties making them superior to inorganics for specific applications. They can, for instance, be processed via simple deposition techniques like thermal evaporation, spincoating or printing. Compared to inorganics, no lattice matching of the used materials is required so that deposition on almost any kind of substrate (e.g. glass or flexible plastic foils) is feasible. This offers the possibility to fabricate bendable[4] as well as translucent electrical devices[5,6]. Since an almost unlimited number of organic compounds is available and properties of these materials can quite easily be changed, for instance by modifying or adding side groups[7], it is conceivable to provide tailored materials with all kinds of functionalities.

In the early days the performance of organic devices was quite limited since intrinsic

[1] Only the abbreviations commonly used for organic semiconductors are mentioned throughout the text. The correct chemical formulae can be found in appendix A, where also the molecular structure for all materials used for experiments in this work is depicted.

organic layers exhibit very low charge carrier densities as well as low mobilities. After introducing the concept of electrochemical doping, as it is commonly used for inorganic devices, the performance of organic components could be enhanced significantly. Efficient state-of-the-art devices like small molecule organic solar cells, as well as organic light emitting diodes, are often realized by employing p-i-n structures where an intrinsic layer is sandwiched between n- and p-doped transport layers[8,9].

For electrochemical doping various concepts have been reported in literature. As first demonstrated by Shirakawa in 1977 for Polyacetylene[10], exposure to oxidizing gases like iodine, oxygen or bromine can lead to an increase of conductivity due to p-type doping[11–14]. Because for n-type doping materials with very high lying HOMO levels are required, which are very unstable against oxygen, it is more difficult to find suitable materials[8]. One approach is the use of alkali metals like lithium or cesium. They are normally deposited as a very thin film between the organic layer and the metal cathode[8,15–17], but can also be co-evaporated with the organic host material[18]. Since such small dopants can easily diffuse through the device, problems regarding stability and processability can occur[17,19].

Therefore, another approach, which leads to better device stability[8], is introducing organic molecular dopants, most commonly via co-evaporation with the organic host material. Several molecular dopants have been successfully applied in the past. Molecules used for n-type doping are, for example, TTN[20] or $CoCp_2$[21]. For p-type doping, for instance, DDQ, TCNQ[22] or F_4-TCNQ were applied, with the latter being the most prominent one. F_4-TCNQ was shown to be a very efficient dopant for a various organic materials like 1-TNATA[23], ZnPc[24], m-MTDATA[25] or VOPc[26]. Nonetheless, it turned out that F_4-TCNQ is quite inefficient for doping wide-band gap materials with very deep lying HOMO levels like CBP, α-NPD or TCTA[23]. This is probably due to the fact that the HOMO levels of these materials are significantly higher than the LUMO of F_4-TCNQ (5.24 eV[24]). Instead, transition metal oxides (TMOs) like WO_3[27], ReO_3[28], or MoO_3[29,30] were found to be a suitable material class for efficient p-type doping of materials because of their very deep lying LUMO levels.

The control of the doping process and other improvements like introducing new device architectures and materials have led to very efficient organic devices. For example, white OLEDs were recently reported to achieve over $100\ \mathrm{lm/W}$ at $1000\ \mathrm{cd/m^2}$[31]. Nonethe-

less, there is still a lack of detailed understanding of the fundamental processes which take place in organic devices.

1.1 Motivation

Although for inorganic semiconductors doping concentrations in the range of ppm are commonly used, the doping concentrations employed in organic devices are usually much higher. When F_4-TCNQ is used as dopant, a few mol% are typically applied[24,25], whereas for TMOs even up to several ten mol% doping concentration are employed[27–29,32]. It is not well understood why such high doping concentrations are needed, because a comprehensive and detailed understanding of the doping process in organic semiconductors is still missing.

For various organic-organic and organic-inorganic material systems the free charge carrier density was determined with different measurement techniques. From the charge carrier density, the doping efficiency, defined as the number of free charge carriers compared to the number of incorporated dopant molecules, can be calculated. The doping efficiency was determined for a variety of different material systems and very low doping efficiencies in the range of only a few per cent were often reported.

For polymer-small molecule systems like P3HT[33] or MEH-PPV[34] doped with F_4-TCNQ doping efficiencies of $5\ \%$ and $1\ \%$, respectively, were determined from impedance spectroscopy measurements. A low doping efficiency was also found for the small molecule-based systems α-NPD doped with $Mo(tfd)_3$ or F_4-TCNQ where impedance spectroscopy revealed a doping efficiency of $3.7\ \%$ and $0.9\ \%$, respectively[35].

In the present thesis, the material system CBP doped with MoO_3 is examined. As depicted in Figure 1.1, the HOMO of CBP ($6.23\ \mathrm{eV}$[36]) is slightly higher than the LUMO-level of MoO_3 ($6.7\ \mathrm{eV}$[36]). Therefore, an efficient charge transfer would be expected between these two materials. The values in this energy diagram were determined by ultraviolet photoelectron spectroscopy (UPS) and inverse photoemission (IPES) measurements[36]. It was found that the Fermi level shifts towards the HOMO edge with increasing doping concentration and IV measurements revealed that the conductivity increases for increasing doping concentrations[36]. Up to that point all results are expected for a doped system, but also for this material system the doping efficiency, which was determined via Kelvin-

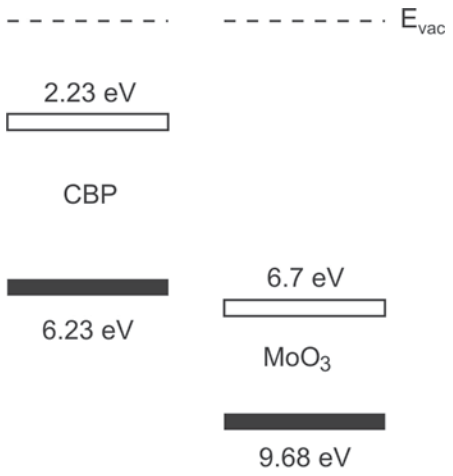

Figure 1.1: Energy levels of neat CBP and MoO_3 measured with UPS and IPES[36].

Probe analysis, turned out to be surprisingly low ($\approx 1-2\ \%$[37]). Similar results were for found for spiro-CBP doped with MoO_3 using capacitance-voltage analysis and polaron induced optical absorption[38] which revealed doping efficiencies of $2\ \%$ - $4.5\ \%$.
The commonly used assumption, that it is sufficient for effective p-type doping that the HOMO level of the dopant is higher than the LUMO of the matrix of course neglects various effects and can also not explain why doping efficiencies for doped organic semiconductors are often found to be unexpectedly low. Factors influencing the doping process which are normally not taken into account might be of structural or electronic origin.
From an energetic point of view the above mentioned picture is very simplified, since the knowledge of the energy levels of the single materials does not provide sufficient information about the electronic structure at the interface, for instance about the formation of interface dipoles. To gain information about the energetics at contacts between two materials, UPS and IPES measurements can be applied (see section 4.2.1). As will be explained in more detail in section 2.3.2 and 4.2.2.1 intermolecular hybridization, which leads to the formation of charge transfer complexes, might also change the energetic conditions at the interface in such a way that charge transfer is not as likely to occur as it would be expected on first sight and might also cause bound charge carriers at the interfaces which cannot contribute to the current flow.
It is well known that also morphological issues play a role when discussing electronic and electrical properties of organic semiconductors. For example, for crystalline and

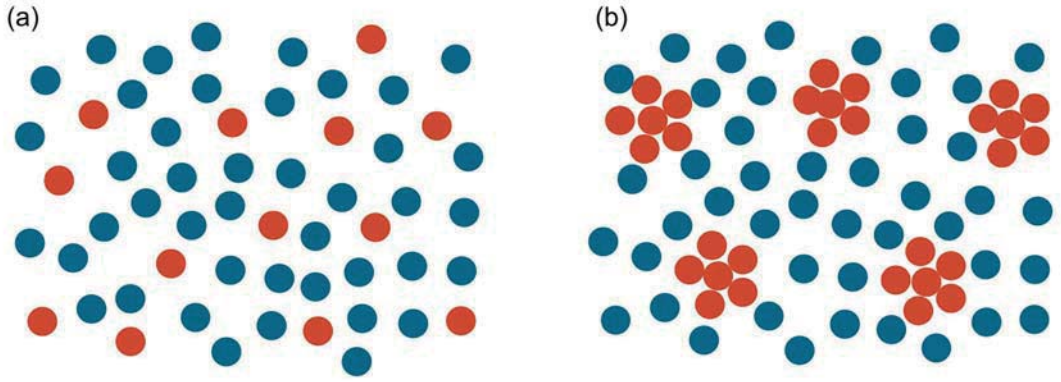

Figure 1.2: (a) Homogeneously dispersed molecules of two co-evaporated materials. (b) Agglomeration of dopants (red) could explain the low doping efficiency found for various material systems.

amorphous materials entirely different models have to be applied to describe the charge transport[39]. However, what is normally not taken into account is the potential influence of the topology. Instead it is commonly thought that by co-evaporation of two materials, for electrochemical doping or incorporation of dyes, the molecules of both components are dispersed homogenously, as schematically shown in Figure 1.2 (a). But it might also be that, depending on the material system, this assumption is wrong and agglomeration of the dopants occurs. As schematically depicted in Figure 1.2 (b) only a fraction of the dopants would then be in contact with the matrix molecules and only for these a charge transfer would be expected. Further analysis of the doping mechanisms and the correlation of morphology and electronic properties is crucial to improve device performance. Therefore, the present thesis tries to shine some light on the issue of low doping efficiencies with the intention to correlate structural with electronic and electrical properties.

1.2 Outline

The present work is organized as follows. In section 2 the theoretical background necessary to understand this thesis is presented. Chapter 3 describes the integrated UHV system where devices and thin films were prepared and where most of the measurements

presented in this thesis were conducted. Following, a brief introduction to all measurement methods used throughout this work is given and the sample preparation is depicted. Chapter 4 shows experimental results of MoO_3-doped CBP thin films. In section 4.1 the topology of the doped films is investigated using different measurement techniques of transmission electron microscopy (TEM), i.e. bright-field TEM, TEM spectroscopy and electron tomography to gain information about the distribution of the MoO_3 dopants within the CBP matrix. Furthermore, it is investigated to what extent the topology can be controlled by changing the substrate temperature during the evaporation process. The section ends with a description of the growth process of the observed MoO_3 agglomerations. Next, the results obtained from FTIR and XPS measurements acquired by Maybritt Kühn and Tobias Glaser within the scope of their respective diploma and PhD theses are summarized to gain insight into the electronic properties of CBP-films doped with MoO_3 (section 4.2). In section 4.3, the influence of the topology on the electrical properties is studied by measuring the IV characteristics of hole-only devices. To probe a possible electrical anisotropy, measurements perpendicular and parallel to the growth direction of the thin films are conducted for different doping concentrations. Furthermore, activation energies of doped films are determined from cryo-IV measurements and the influence of the substrate temperature onto the electrical properties is examined. By correlating the structural, electronic and electrical measurements, a model to describe the charge transport of MoO_3-doped CBP films is presented in section 4.4. In chapter 5, the influence of the deposition angle on the performance of OLEDs is investigated and in particular the organic/LiF interface is analyzed. The thesis is concluded with a short summary and an outlook on possible future work in chapter 6.

2 Theoretical Background

In the following chapter, the theoretical background, needed to understand the present thesis, will be presented. The chapter starts with an introduction to organic semiconductors, followed by the basic theory of charge transport in disordered organic semiconductors and models used to describe the doping process. Next, expressions to describe the IV characteristics of unipolar devices are presented and charge injection for different kinds of interlayers is elaborated. Finally, basic theory about OLEDs is depicted.

2.1 Organic Semiconductors

Organic semiconductors are based on carbon compounds with conjugated double bonds. In such systems, usually sp^2-hybridization occurs to minimize bond energies. One s-orbital, as well as two p-orbitals (p_x and p_y), form three mixed orbitals, which arrange in one plane with an angle of $120°$ to each other, while the fourth valence electron of the carbon atom occupies the p_z-orbital, which is oriented perpendicular to that plane. In a molecule, the sp^2-orbitals of neighboring molecules form so-called σ-bonds. Due to the strong orbital overlap, large splitting into binding σ- and antibinding σ^*-orbitals occurs, where electrons are highly localized. Figure 2.1 (a) depicts the energy levels in the case of sp^2-hybridization. As an example for an organic molecule, a schematic drawing of the hybrid orbitals of benzene is shown in Figure 2.1 (b). No interaction with radiation in the visible spectral range can take place, since the energy difference of occupied σ- and unoccupied σ^*-orbitals is too high. By contrast, superposition of the p_z-orbitals leads to weak, conjugated π-bonds. Because of the low binding energy of these bonds, electrons are delocalized along the whole conjugation length. Due to the weak overlap of the p_z-orbitals, only minor splitting of the p_z-states occurs and binding π- and antibinding π^*-orbitals are formed. The highest occupied π-state of a molecule is commonly denoted as HOMO (highest occupied molecular orbital), whereas the lowest unoccupied π^*-orbital is called LUMO (lowest unoccupied molecular orbital). Since the energy gap between

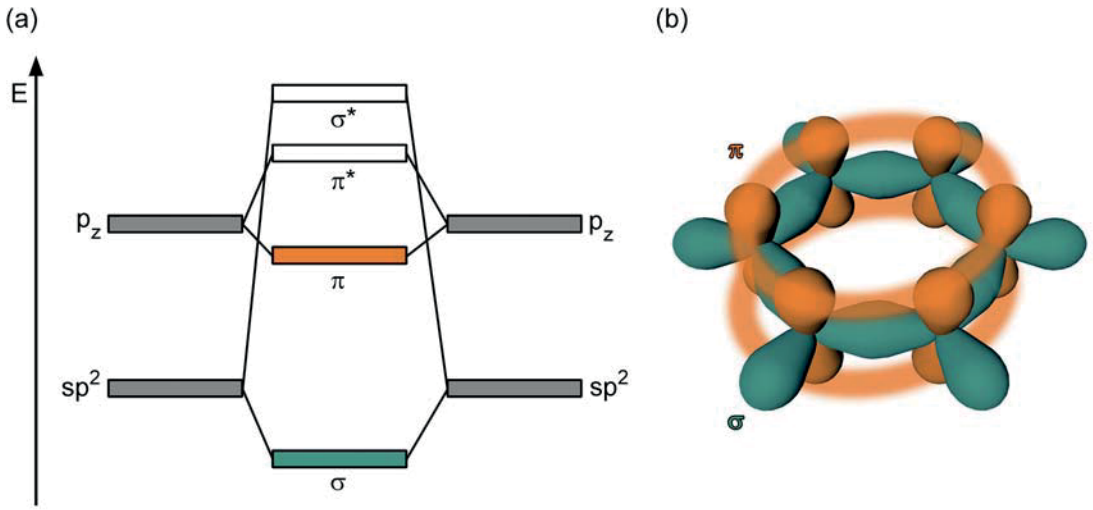

Figure 2.1: (a) Schematic illustration of the binding- and antibinding states in an organic molecule.
(b) Schematic drawing of the hybrid orbitals of benzene with σ- and π-bonds. The sp^2-hybridized orbitals form so-called σ-bonds, while the p_z-orbitals are only weakly bound via π-bonds.

HOMO and LUMO lies in the range of several eV, it covers the visible part of the optical spectrum and makes organic semiconductors suitable for optical applications like OLEDs or organic solar cells.

2.2 Theory of Charge Transport in Disordered Organic Semiconductors

The present section will give an overview of different models, which were developed to describe charge transport in amorphous organic semiconductors. To a great extent it follows the outline taken in Ref. [40].
In well ordered systems, like inorganic semiconductors or to a certain extent also organic crystals, band transport takes place. In contrast, only weak intermolecular coupling between the molecules exists in disordered amorphous semiconductors. Therefore, no band formation occurs, but instead charge transport proceeds via so called hopping transport between adjacent molecules. This process requires thermal activation to overcome energy

differences between different sites[40]. The mobility μ is related to the activation energy E_a, the temperature T and the Boltzmann constant k via[41]

$$\mu \propto \exp(-E_a/kT). \tag{2.2.1}$$

A basic model to describe hopping transport is the so-called Gaussian disorder model (GDM) introduced by Bässler[42]. An array of uncorrelated hopping sites with a cubic symmetry is considered. The energy ϵ of each site is given by a Gaussian density of states (DOS) with variance σ[42]:

$$D(\epsilon) = \frac{1}{\sqrt{2\pi\sigma^2}} \exp\left(-\frac{\epsilon^2}{2\sigma^2}\right). \tag{2.2.2}$$

σ is a measure for the amount of disorder and is mainly due to fluctuations of the lattice polarization energies in the case of small molecule systems[42].
The hopping rate ν_{ij} between the sites i and j can be described in different ways, with the most simple one being the so-called Miller-Abrahams form[40,42,43]

$$\nu_{ij} = \nu_0 \exp\left(-2\gamma a \frac{\Delta R_{ij}}{a}\right) \begin{cases} \exp\left(-\frac{\epsilon_j - \epsilon_i}{kT}\right) & \text{if } \epsilon_j > \epsilon_i, \\ 1 & \text{if } \epsilon_j \leq \epsilon_i. \end{cases} \tag{2.2.3}$$

with a pre-factor ν_0, the average lattice distance a, the inverse localization radius between adjacent sites γ, the distance between the sites i and j denoted as ΔR_{ij} and the temperature T.
Additionally, the so called positional disorder, described by the parameter Σ, must be considered. Σ is due to variation of intersite distances and variation in coupling of adjacent molecules due to different mutual molecule orientations[42]. The charge carrier mobility μ can be expressed in dependence of the temperature T, the electric field E and the two disorder parameters σ and Σ by[42]:

$$\mu(\sigma, \Sigma, E, T) = \mu_0 \exp\left(-\frac{4\widehat{\sigma}^2}{9}\right) \begin{cases} \exp\left(C(\widehat{\sigma}^2 - \Sigma^2)\sqrt{E}\right) & \text{if } \Sigma \geq 1.5, \\ \exp\left(C(\widehat{\sigma}^2 - 2.25)\sqrt{E}\right) & \text{if } \Sigma \leq 1.5. \end{cases} \tag{2.2.4}$$

with $\widehat{\sigma} = \sigma/kT$ and the constant C, which depends on the site separation[40].
According to equation (2.2.4), charge carriers might also move against the field direction, since for $\widehat{\sigma} < \Sigma$ respectively $\Sigma > 1.5$ the mobility becomes negative. This effect, which can only occur at low electric fields, is due to an interplay between positional disorder Σ and energetic disorder σ, leading to situations where this behavior is energetically favorable[40,44].
The electrical field dependence can be described by a Poole-Frenkel like behavior of the form $\mu \propto \exp\sqrt{E}$. Experimentally, this Poole-Frenkel like dependence was found to be valid for a wider range of electrical fields than predicted by equation (2.2.4). To account for this deviation, Gartstein and Conwell introduced the so called correlated Gaussian disorder model (CGDM), where additionally spatial correlation of the energetic disorder is assumed which is due to dipole interactions of charged species with adjacent sites[45].
Charge carriers relax towards the tail states of the DOS and tend to occupy a so-called occupational-DOS (ODOS) in quasi-equilibrium. The center of this ODOS is displaced by $\varepsilon_0 = \sigma/kT$ from the maximum of the DOS[46,47] (see Figure 2.2 (a)). For small carrier densities, the Fermi energy E_F is located deep in the band gap, well below σ/kT, and does therefore not play a role for charge transport. Since the transport energy E_t is located close to the maximum of the DOS, the activation energy equals approximately σ/kT and is independent of the charge carrier density (see Figure 2.2 (a)). In conjunction with equation (2.2.1) this results in a non-Arrhenius-like dependence of the mobility with respect to the temperature, namely $\log\mu \propto 1/T^2$ [40,42].